

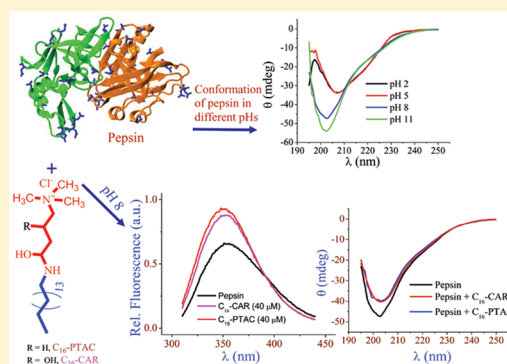
Solution Behavior and Interaction of Pepsin with Carnitine Based Cationic Surfactant: Fluorescence, Circular Dichroism, and Calorimetric Studies

Subhajit Ghosh, Subhrajyoti Dolai, Trilochan Patra, and Joykrishna Dey*

Department of Chemistry, Indian Institute of Technology Kharagpur, Kharagpur - 721 302, India

S Supporting Information

ABSTRACT: The present work reports the pH-induced conformational changes of pepsin in solution at room temperature. The conformational change makes the protein surface active. The protein was found to be present in the partially denatured state at pH 8 as well as at pH 2. The fluorescence probe and circular dichroism (CD) spectra suggested that the most stable state of pepsin exists at pH 5. The binding affinities of pepsin in its native and denatured states for a D,L-carnitine-based cationic surfactant (3-hexadecylcarbamoyl-2-hydroxypropyl)trimethylammonium chloride (C_{16} -CAR) were examined at very low concentrations of the surfactant. The thermodynamics of the binding processes were investigated by use of isothermal titration calorimetry. The results were compared with those of (3-hexadecylcarbamoylpropyl)trimethylammonium chloride (C_{16} -PTAC), which is structurally similar to C_{16} -CAR, but without the secondary -OH functionality near the headgroup. None of the surfactants were observed to undergo binding with pepsin at pH 2, in which it exists in the acid-denatured state. However, both of the surfactants were found to spontaneously bind to the most stable state at pH 5, the partially denatured state at pH 8, and the alkaline denatured state at pH 11. Despite the difference in the headgroup structure, both of the surfactants bind to the same warfarin binding site. Interestingly, the driving force for binding of C_{16} -CAR was found to be different from that of C_{16} -PTC at pH \geq 5. The steric interaction of the headgroup in C_{16} -CAR was observed to have a significant effect on the binding process.



1. INTRODUCTION

Protein–surfactant interaction is very important in protein isolation and purification processes.^{1,2} Also, because of its relevance to detergent, pharmaceutical, and food industry, protein–surfactant interaction has attracted tremendous attention in the past few decades.^{3–7} There are some excellent reviews which have summarized the work from time to time.^{8–12} The serum albumins, e.g., human serum albumin (HSA) and bovine serum albumin (BSA), were extensively studied as model proteins.^{13–15} Other proteins like hemoglobin, myoglobin, casein, and lysozyme have also been investigated.^{16,17} One of the most used surfactants for these studies has been sodium dodecyl sulfate (SDS), which is a commonly used anionic surfactant in the industry. In most of the earlier reports, interaction of BSA with SDS and the structure of BSA/SDS complex are discussed. The study of the interaction of SDS with trypsin and papain is also reported in the literature.^{18–20} Other anionic surfactants whose interactions with proteins have been investigated are sodium dodecylbenzenesulfonate (SDBS), sodium laurate (SL), etc.²¹ These studies have shown that surfactant binding to protein results in either partial unfolding of the protein or complete denaturation even at a concentration much less than its critical micelle concentration (CMC).²² In general, surfactant molecules interact with the protein through various forces including van

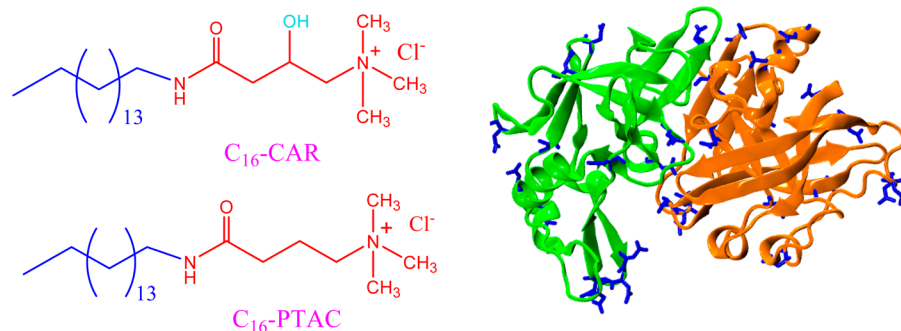
der Waals, H-bonding, hydrophobic, and electrostatic interaction.²³

Although the interactions of various proteins with anionic surfactants are widely studied in the literature, there are only a few reports on the studies of binding of cationic surfactants to proteins.²⁴ Sun et al. studied the interaction of cetylpyridinium bromide (CPB) with BSA in pH 7 buffer and observed that binding of CPB at low concentration unfolds the protein but, in the presence of a high concentration of CPB, BSA refolds.²⁵ Another investigation on the interaction of dodecyltrimethylammonium bromide (DTAB), tetradecyltrimethylammonium bromide (TTAB), cetyltrimethylammonium bromide, and cetylpyridinium chloride with BSA also demonstrated stabilization of the protein structure, and an effect of the surfactant headgroup on the protein–surfactant interaction was noted.²⁶ Interaction of BSA with cationic surfactants of different chain lengths was also studied by Kun et al., who showed that both hydrophobic and electrostatic interactions play a role in the stabilization of BSA/surfactant complex.²⁷ Recently, interaction of gemini surfactants with globular proteins has been reported.^{28–31}

Received: July 23, 2015

Revised: September 8, 2015

Published: September 8, 2015

Chart 1. Chemical Structures of Cationic Surfactants, C₁₆-CAR and C₁₆-PTAC, and X-ray Crystal Structure of Pepsin

Like serum albumins, pepsin (see Chart 1 for structure) is a small (35 kDa) globular protein with 327 amino acid residues.^{32,33} Pepsin is a proteolytic enzyme, which catalyzes the hydrolysis of peptide bonds of most proteins, except carbohydrate-rich proteins, preferably between two aromatic amino acids (e.g., Phe-Phe and Phe-Tyr). There are many uses of proteolytic enzymes in detergent industry in removal of stains of blood, egg-white, etc., by degradation of the relevant protein into small peptides and amino acids. After the aspartic proteins, e.g., HIV protease and rennin, were linked to human diseases, this group of enzymes attracted a huge interest in order to understand their structure–function relationship. Pepsin with two Asp residues in its active site is a good model for the study of aspartic protease, as detailed information on the structure of the protein is available. Wang and co-workers have reported spectroscopic and thermodynamic studies on the interaction between pepsin and bisphenol A (BPA).³⁴ They observed that hydrophobic and H-bonding interactions and steric effects stabilize the pepsin structure. Also, BPA was found to bind pepsin in the cleft between the C-terminal and N-terminal lobes.

Although some reports are available on the interactions of small molecules with pepsin,³⁵ there are very limited studies on pepsin–surfactant interaction. Recently, Chakraborty et al. have studied the interaction of CTAB with pepsin at three different pHs.³⁶ They have concluded that, at low concentrations, CTAB electrostatically binds to the negatively charged peripheral sites of pepsin with a concomitant increase in hydrophobicity and imparts stability to the protein structure. Boeris et al., on the other hand, have studied the interaction of the natural polyelectrolyte chitosan with pepsin.³⁷ They found that chitosan does not affect the thermal and chemical thermodynamical stability of the enzyme. These apparently contrasting results led to the present investigation. Herein, we investigate the effect of surfactant binding on the native as well as on the partially denatured state (I_p) of pepsin. We report here the interactions of pepsin with a new carnitine-based cationic surfactant (3-hexadecylcarbamoyl-2-hydroxypropyl)-trimethylammonium chloride (C₁₆-CAR). Unlike CTAB, C₁₆-CAR has a hydroxyl (—OH) group and an amide (—NHC(=O)—) group in the hydrocarbon chain. C₁₆-CAR has been found to spontaneously form a vesicle in aqueous solution above a relatively low CMC value (0.03 mM).³⁸ If the surfactant binding is purely electrostatic in nature, and occurs through the headgroup, these groups are expected to have an effect on the interaction. In order to examine the effect of the —OH group on surfactant binding, we have also investigated the interaction of 3-(hexadecylcarbamoylpropyl)trimethylammonium chloride (C₁₆-PTAC) with pepsin. The latter surfactant has a structure

closely similar to C₁₆-CAR but without the —OH group at the surfactant head. The chemical structures of the cationic surfactants are shown in Chart 1. The effect of the surfactants on the stability of protein in aqueous medium was investigated using steady-state and time-resolved fluorescence and circular dichroism (CD) spectroscopy. The binding forces were determined using isothermal titration calorimetry (ITC). In order to understand the protein–surfactant interaction, we have also studied the solution behavior of pepsin at different pHs.

2. MATERIALS AND METHODS

2.1. Reagents. Porcine pepsin ($M_w = 35$ kDa) was obtained from Sigma (Bangalore, India) and used as received. D,L-Carnitine, 4-*N,N*-dimethylaminobutyric acid, and *n*-hexadecyl amine were from Sigma-Aldrich (Bangalore, India). Dicyclohexyl carbodiimide (DCC), 4-*N,N*-dimethylamino pyridine (DMAP), sodium monohydrogen phosphate, sodium dihydrogen phosphate, and orthophosphoric acid were obtained from SRL (Mumbai) and were used directly from the bottle. The cationic surfactants C₁₆-CAR and C₁₆-PTAC were synthesized in our laboratory. The detailed synthetic procedure and spectroscopic identification of the surfactants are included in the Supporting Information.

2.2. Methods. Surface Tension Measurements. An automated Surface Tensiometer (model 3S, GBX, France) was used to measure the surface tension (γ) using the Du Nuoy ring detachment method. The temperature of the thermostating vessel holder was maintained at 25 °C by a temperature controlled water circulating bath (Julabo, model F12). The platinum–iridium ring was periodically cleaned using 50% (v/v) ethanol/HCl solution and distilled water. The instrument was calibrated before use by measuring the γ value of Milli-Q water (18.2 Ω). A stock solution of the surfactant was made in phosphate buffers (20 mM) of pH 2, 5, 8, and 11, respectively. Pepsin (14 μ M) stock was also made in the respective buffer. Before each measurement started, the solution was thoroughly mixed and allowed to equilibrate for 5 min in the thermostating vessel holder.

Steady-State Fluorescence Measurements. A PerkinElmer LS-55 luminescence spectrometer was used to measure steady-state fluorescence spectra. The spectrometer is equipped with a filter polarizer and a thermostating cell holder. The temperature was controlled within ± 0.1 °C using a circulating bath (Thermo Neslab RTE-7). Pepsin concentration was kept constant at 14 μ M, and surfactant concentration was varied. The surfactant stock solutions were made in appropriate phosphate buffer (20 mM) of pH 2, 5, 8, or 11. Dilution of an aliquot of this afforded surfactant solutions of varying

concentrations. Pepsin solutions were excited at 295 nm in order to minimize the contribution from Tyr, and the spectrum was recorded from 310 to 440 nm. The emission and excitation slits were kept at 2.5 and 3.2 nm. The fluorescence intensity was measured at 350 nm.

The steady-state fluorescence anisotropy (r) of tryptophan (Trp) residue was calculated according to the equation³⁹

$$r = (I_{VV} - GI_{VH}) / (I_{VV} + 2GI_{VH}) \quad (1)$$

where I_{VV} and I_{VH} are the fluorescence intensities respectively polarized parallel and perpendicular to the vertically polarized excitation beam. The software supplied by the manufacturer automatically determined the instrumental grating factor G ($=I_{VH}/I_{HH}$) and fluorescence anisotropy. The excitation and emission slit widths were fixed at 2.5 and 4 nm, respectively. A 350 nm cutoff filter was placed in the emission beam to eliminate the effect of scattered radiation. The r value was measured at an emission wavelength of 360 nm over an integration time of 10 s. An average of five such readings for each sample was taken as the r value.

Time-Resolved Fluorescence Measurements. The fluorescence lifetime of the Trp residues of pepsin was measured by the use of an EasyLife (Optical Building Blocks Corporation, Birmingham, U.K.) instrument, which uses a 295 nm diode laser as the light source and a 305 nm emission cutoff filter. The fluorescence intensity decay curves were fit to a biexponential function using an iterative fitting program provided by the supplier. The best fit was judged by the χ^2 value (0.8–1.2) and the residual plot. For lifetime measurements, pepsin concentration was 14 μM , but C_{16} -CAR and C_{16} -PTAC concentrations were kept at 40 μM at all pHs, except pH 5 in which the concentration of C_{16} -CAR and C_{16} -PTAC was 20 μM .

Circular Dichroism Spectroscopy. The circular dichroism (CD) spectra of protein solutions were measured with a Jasco J-815 spectropolarimeter (Japan) using a quartz cell of 1 mm path length. The temperature of the cell was controlled within ± 0.1 °C using a water circulating bath (Escy Enterprises, India). The spectrum was recorded in the range 190–260 nm. Each spectrum was blank subtracted. For each spectrum, an average of three scans with a speed 50 of nm/min, bandwidth of 1 nm, and response time of 2 s was recorded.

Dynamic Light Scattering. A Zetasizer Nano ZS (Malvern Instrument Lab, Malvern, U.K.) light scattering spectrometer equipped with a He–Ne laser operated at 4 mW ($\lambda_0 \cong 632.8$ nm) at 25 °C, a digital correlator, and a computer-controlled and stepping-motor-driven variable angle detection system was used for the dynamic light scattering (DLS) measurements. For each sample, the data acquisition was made for at least 100 counts and each experiment was repeated at least twice. For protein solutions, the pepsin concentration was fixed at 14 μM . The surfactant concentration was 40 μM for all pHs, except pH 5 in which $[C_{16}\text{-CAR}] = [C_{16}\text{-PTAC}] = 20$ μM . All measurements were performed at 25 °C.

Isothermal Titration Calorimetry (ITC). ITC experiments were carried out in a Microcal iTC₂₀₀ (made in U.S.A.) system at 25 °C at four different pHs, i.e., pH 2, 5, 8, and 11, in phosphate buffer solutions. Titration of C_{16} -CAR and C_{16} -PTAC against pepsin was carried out by injecting C_{16} -CAR or C_{16} -PTAC and the same surfactant against phosphate buffer. The pepsin concentration was kept at 28 μM . The concentration of C_{16} -PTAC and C_{16} -CAR in pH 2, 5, 8, and 11 buffer was 0.5 mM. A total of 20 injections were made at a spacing of 120 s for each titration. A stirring speed of 400 rpm,

a reference power of 5 $\mu\text{cal/s}$, and an initial delay of 60 s were used for all titrations. For all measurements, the cell temperature was maintained at 25 °C.

3. RESULTS AND DISCUSSION

3.1. Solution Behavior of Pepsin. As mentioned before, proteolytic enzymes, such as pepsin, can be used with detergent for the removal of stains of blood, egg-white, etc., by degradation of the relevant protein into oligopeptides and amino acids. Therefore, before its interaction with the detergent molecule can be understood, the solution behavior of pepsin should be investigated. The detergent solutions are normally mildly alkaline in nature. However, pepsin is known to be stable only in acidic pH and it undergoes denaturation in basic pH (>8), thereby making the protein structure more flexible.⁴⁰ This means that the enzymatic activity of pepsin should be maintained only in acidic pH. The flexibility of the protein structure can be examined by measuring its surface activity. The surface activity of proteins is not only due to the percent distribution of polar and nonpolar amino acid residues on its surface, but it is also related to its molecular flexibility and/or conformational stability at the air/water interface.⁴¹ The molecular flexibility is important in facilitating orientation and spreading at an interface, forming cohesive interfacial films. In fact, the surface activity of proteins is an important consideration in food industry, as most foods are either emulsions or foams, which are normally stabilized by low-molecular-weight surfactants.

It is well-known that the pI of pepsin is 1,⁴² which means it is uncharged at pH 1 and negatively charged at higher pHs. In order to test whether pepsin itself has any surface activity or not, we measured the surface tension, $ST(\gamma)$, of an aqueous solution of fixed concentration of pepsin at different pHs. The plot of variation of γ with pH is presented in Figure 1. It can be

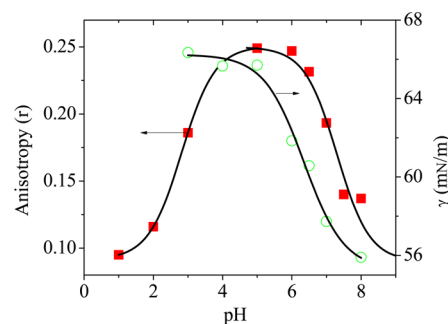


Figure 1. Plot of fluorescence anisotropy (r) (filled squares) and surface tension (γ , mN/m) (open circles) of pepsin solution ($C_p = 14$ μM) as a function of pH at 25 °C.

observed that, at low pH, it has almost no surface activity, but with the increase in pH, the γ -value of water gradually decreases, suggesting that in the denatured state pepsin behaves like a surface-active agent. This must be associated with the ionization of the buried Asp residues at pH > 5 , resulting in denaturation of the protein. This is supported by the large negative zeta-potential value of pepsin at pH 8 (-10.64 ± 0.86 mV) compared to that at pH 2 ($+0.56 \pm 0.12$ mV). The pH above which the protein undergoes conformational change is ca. 6.5, which is closely equal to that reported in the literature.⁴⁰ This means that the pK_a value of the $-\text{COOH}$ group of the Asp side chain is 6.5. The results obtained from ST studies thus

Table 1. Time-Resolved Fluorescence Data of Pepsin and Pepsin/Surfactant Complexes in 20 mM Phosphate Buffer (pH 2, 5, 8, and 11) at 25 °C^a

pH	substances	τ_1/ns (f_1)	τ_2/ns (f_2)	$\langle\tau_i\rangle/\text{ns}$	χ^2
2	pepsin	5.18 ± 0.11 (0.116 ± 0.016)	2.61 ± 0.08 (0.883 ± 0.016)	2.90 ± 0.15	0.93
	pepsin/C ₁₆ -PTAC	5.30 ± 0.10 (0.130 ± 0.001)	2.49 ± 0.04 (0.871 ± 0.001)	2.85 ± 0.03	1.16
	pepsin/C ₁₆ -CAR	5.12 ± 0.04 (0.128 ± 0.002)	2.36 ± 0.04 (0.872 ± 0.003)	2.71 ± 0.02	0.91
5	pepsin	6.02 ± 0.45 (0.103 ± 0.003)	3.03 ± 0.26 (0.896 ± 0.004)	3.33 ± 0.12	0.95
	pepsin/C ₁₆ -PTAC	5.26 ± 0.40 (0.156 ± 0.015)	1.89 ± 0.25 (0.858 ± 0.019)	2.28 ± 0.18	0.98
	pepsin/C ₁₆ -CAR	5.40 ± 0.20 (0.129 ± 0.003)	2.13 ± 0.15 (0.870 ± 0.005)	2.54 ± 0.08	1.11
8	pepsin	4.41 ± 0.19 (0.118 ± 0.028)	2.85 ± 0.32 (0.882 ± 0.028)	3.03 ± 0.26	1.16
	pepsin/C ₁₆ -PTAC	4.24 ± 0.14 (0.161 ± 0.009)	3.04 ± 0.19 (0.839 ± 0.009)	3.23 ± 0.09	0.88
	pepsin/C ₁₆ -CAR	4.10 ± 0.03 (0.151 ± 0.011)	2.73 ± 0.30 (0.849 ± 0.012)	2.94 ± 0.13	0.85
11	pepsin	3.92 ± 0.64 (0.142 ± 0.018)	2.55 ± 0.84 (0.858 ± 0.019)	2.74 ± 0.39	0.91
	pepsin/C ₁₆ -PTAC	3.78 ± 0.41 (0.154 ± 0.009)	2.37 ± 0.63 (0.845 ± 0.009)	2.58 ± 0.29	1.13
	pepsin/C ₁₆ -CAR	3.26 ± 0.14 (0.239 ± 0.011)	2.36 ± 0.10 (0.760 ± 0.025)	2.57 ± 0.08	1.14

^aConcentrations: [C₁₆-CAR] = [C₁₆-PTAC] = 40 μM for pH 5, [C₁₆-CAR] = [C₁₆-PTAC] = 20 μM for pH 2, 8, and 11.

indicate that flexibility of pepsin increases with the increase of pH above 5, which is consistent with its denaturation at alkaline pH.

In support to the above conclusion, we have measured the intrinsic fluorescence spectrum (Figure S5) of pepsin at different pHs. The intrinsic fluorescence of pepsin is due to the five Trp residues (Trp-39, Trp-141, Trp-181, Trp-190, and Trp-300) in the polypeptide chain. The conformational change is clearly manifested by the change in fluorescence spectrum of Trp residues in going from pH 2 to 11. As shown in Figure S5, the intensity of the fluorescence spectrum increases in going from pH 2 to 5, but it decreases upon further increase of pH. It is believed that, at low pH, the protonated imidazole ring and carboxyl group of the His moiety quench the fluorescence of Trp and Tyr moieties internally.³⁶ However, the observed fluorescence quenching in alkaline pH is accompanied by the reduction of fluorescence lifetime (see data in Table 1), suggesting occurrence of either dynamic quenching or conformational change of the protein. The red-shift of the fluorescence spectrum at pH 5, 8, and 11 ($\lambda_{\text{max}} = 354$ nm) relative to that at pH 2 ($\lambda_{\text{max}} = 349$ nm) is indicative of the change of the microenvironment of Trp residues as a consequence of conformational change of the protein.

To examine the increase of the molecular flexibility of pepsin with the change of pH, we measured the steady-state fluorescence anisotropy (r) of the Trp residue of pepsin, which is sensitive to change in rigidity of the microenvironment. The variation of r with pH is shown by the bell-shaped plot in Figure 1. The maximum r -value is observed at pH 5 which decreased significantly on both sides. The data in Figure 1 suggest that at pH 5 the Trp residues on both N- and C-terminal lobes are in a rigid microenvironment corresponding to the tightly packed native state (N_p). In the N_p state, both the N- and C-terminal lobes are tightly folded. On the other hand, the molten globule-like denatured state which is loosely packed shows a significant decrease of the r -value of Trp residues. The small value of r at pH 8 is associated with the I_p state in which the N-terminal lobe is partially unfolded and the C-terminal lobe is tightly folded.³³ The partial unfolding of the N-terminal lobe must be a consequence of deprotonation of the -COOH groups of some buried Asp residues which occurs at pH > 5 and Trp residues are exposed to bulk water. Indeed, the conformational change of pepsin in this pH region is also reported by others.⁴⁰ The decrease of r -value below pH 5, on the other hand, can be linked to the titration of His-53 in the

N-terminal lobe. The protonation of the His-53 residue ($pK_a \sim 3.0$) results in a partial unfolding of the N-terminal lobe, producing an acid-denatured state, D_p . This means that, in both acid- and alkali-induced denaturation, only the N-terminal lobe is unfolded. In other words, the C-terminal lobe of pepsin is very stable. The stability of the C-terminal lobe against heat and proteolytic digestion compared to the N-terminal lobe in the N_p state has also been reported elsewhere.⁴³

That the alkali-induced denaturation of the N-terminal lobe occurs as a result of deprotonation of -COOH group(s) of the buried Asp residue(s) ($pK_a \sim 6.5$) can be shown by the large negative zeta-potential value of the I_p state as discussed above. The ζ -potential value becomes less negative (-3.94 ± 0.04 mV) in the N_p state and decreases further with the protonation of the His-53 residue at pH < 5 and finally becomes slightly positive in the D_p state at pH 2 ($+0.56 \pm 0.12$ mV).

In order to confirm the conformational changes of pepsin upon pH variation, we have measured the CD spectra of the protein under different conditions. CD spectra are usually used to elucidate the global picture of protein structure.⁴⁴ Although CD cannot provide a detailed structure of the protein, it provides the fraction of α -helix, β -sheet, and random coil. The conformational change of the protein in the pH region 2–8 is clearly reflected by the change in CD spectrum, as shown in Figure 2. It is observed that the CD spectrum at pH 5 corresponding to the N_p state contains one minimum at 207 nm, which has shifted to 202 nm at pH 8 with the partial loss of helicity. In the N_p state at pH 5, α -helix content is 3.9% and β -sheet percentage is 65.6%, suggesting that pepsin is a β -sheet-rich protein. At pH 8, where the protein is in the I_p state, the

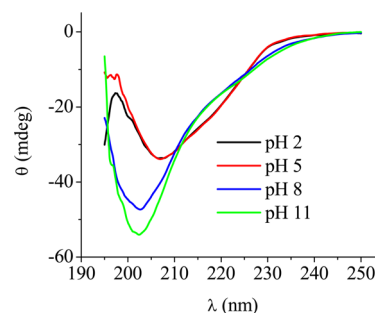


Figure 2. CD spectra of pepsin (14 μM) in phosphate buffer (20 mM) of pH 2–11 at 25 °C.

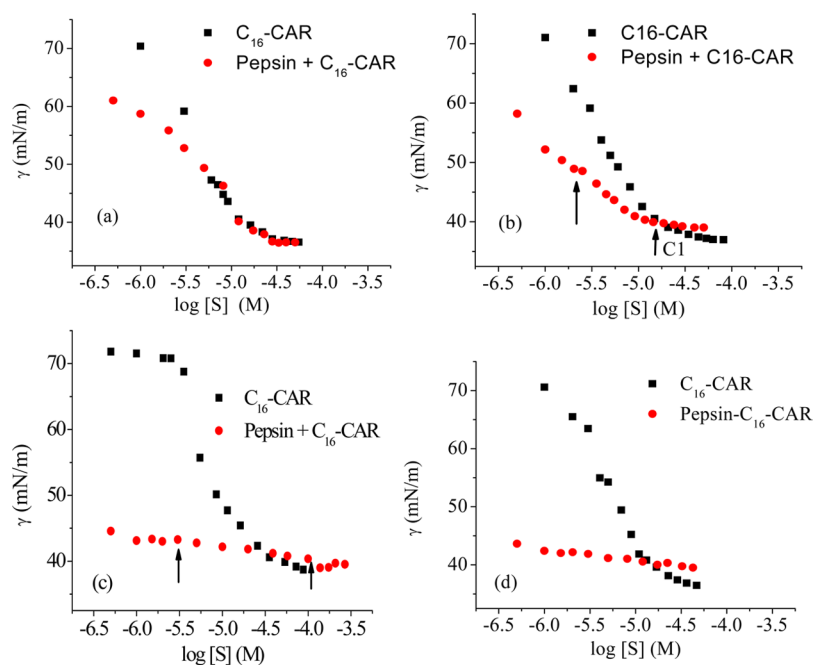


Figure 3. Plots of surface tension (γ) of phosphate buffer (20 mM) as a function of $[C_{16}\text{-CAR}]$ in the absence and presence of pepsin ($C_p = 14 \mu\text{M}$): (a) pH 2, (b) pH 5, (c) pH 8, and (d) pH 11 at 25 °C.

percentage of α -helix decreased to 0% and the β -sheet percentage decreased to 55.8%. The percentages of the turn and unordered structure, on the other hand, increased, indicating denaturation of the protein. This suggests a large conformational change of the pepsin at higher pH. In fact, in extreme alkaline (pH 11) solution, the helicity is completely lost and the CD spectrum corresponds to a random denatured structure of pepsin. Similarly, in aqueous solution of pH 2, the α -helix (2.6%) as well as β -sheet content (67.5%) is decreased in comparison to that in pH 5 solution, which must be associated with the conformational change of the N-terminal lobe of the protein.

3.2. Interaction of Pepsin with $C_{16}\text{-CAR}$ and $C_{16}\text{-PTAC}$.

Surface Tension Studies. Pure $C_{16}\text{-CAR}$ molecules in buffer solution are preferentially adsorbed at the air/water interface due to their amphiphilic character,³⁸ reducing the cohesive interaction of water molecules at the interface. Consequently, the γ -value of water is reduced on successive addition of the $C_{16}\text{-CAR}$ surfactant until saturation of the interface. The threshold point at which the saturation of the interface occurred is called the CMC. The profiles of pure $C_{16}\text{-CAR}$ at pH 2, 5, 8, and 11 are shown in parts a, b, c, and d of Figure 3, respectively. The CMC values of $C_{16}\text{-CAR}$ at pH 2, 5, 8, and 11 as obtained from respective ST plots are 28, 26, 33, and 27 μM , respectively. Since the surfactant molecule does not have any ionizable functional group, the small but measurable difference in the CMC values in different pHs is due to the difference in the ionic strength of the phosphate buffers at the pH employed.

When there is a strong interaction present between the protein and surfactant, the surface tension curve of the protein/surfactant mixture is expected to deviate from that of the surfactant itself. Figure 3 shows the ST plots of $C_{16}\text{-CAR}$ in the absence and presence of a constant concentration of pepsin. At pH 2, pepsin is positively charged and is in its native state. From Figure 3a, we can see that the interaction of $C_{16}\text{-CAR}$ and pepsin is weak at pH 2. The γ vs $\log[S]$ plots of pure $C_{16}\text{-CAR}$ and in the presence of pepsin coincide after a certain

concentration of the surfactant, suggesting a weak or no interaction between the $C_{16}\text{-CAR}$ and pepsin at pH 2. At pH 5, pepsin is most stable and is in a non-native state. In this state, when $C_{16}\text{-CAR}$ interacts with pepsin, the ST profile deviates from that of pure $C_{16}\text{-CAR}$. Thus, the ST profile of pepsin/ $C_{16}\text{-CAR}$ shows two break points indicated by upward arrows. The first break point is around 2 μM which corresponds to the displacement of pepsin from the air/water interface or interaction of pepsin with $C_{16}\text{-CAR}$. The concentration corresponding to this break point is called the critical association concentration (CAC). The second break point termed C_1 appears at $\sim 15 \mu\text{M}$, which is less than the CMC value of $C_{16}\text{-CAR}$ itself. This means that the adsorption of a positively charged $C_{16}\text{-CAR}$ molecule to the pepsin makes the resulting pepsin/ $C_{16}\text{-CAR}$ complex charge neutral, and as a result, the hydrophobicity of the complex increased and therefore $C_1 < \text{CMC}$. In pH 8 buffer, pepsin is in the I_p state and the γ - $\log[S]$ plot also shows two break points indicated by upward arrows. In the I_p state, the charge density in the surface increases, and the surface activity of the pepsin also increases. Therefore, an increase of pH from 5 to 8 increased the interaction of pepsin with $C_{16}\text{-CAR}$. This must be due to the structural change of the pepsin molecule at higher pH. Thus, pepsin in the I_p state interacts more strongly with $C_{16}\text{-CAR}$. At pH 11, the pepsin is in a complete denatured state and, as it has polyelectrolyte nature, it shows high surface activity at this pH. The addition of $C_{16}\text{-CAR}$ to the pepsin solution does not change γ significantly, and it is difficult to predict from the ST profile whether $C_{16}\text{-CAR}$ molecules bind to pepsin or not at this pH.

Steady-State Fluorescence Spectra. Fluorescence spectroscopy is a powerful tool to study protein–ligand interaction. The intrinsic fluorescence of a protein can give us valuable information about the protein structure and dynamics, and can be used to study the folding/refolding of protein and association/dissociation processes of ligand. The steady-state fluorescence spectra can also give information about the local

microenvironment in and around the Trp residue. Pepsin contains five Trp residues, but all five residues, however, are not exposed to the bulk water. Some of the residues are buried and are nonfluorescent. To envision the pepsin–surfactant interactions, we have measured fluorescence spectra of pepsin at four different pHs, pH 2, where the protein is in its native state, pH 5, where pepsin is in its most stable state, pH 8, where protein is in the I_p state, and pH 11, where the protein is in the complete denatured state. Additionally, the interactions of the two different states of pepsin with two structurally similar surfactant molecules were studied to have a better insight into the protein–surfactant interaction.

Figure S6 shows the fluorescence spectra of pepsin alone as well as in the presence of C_{16} -PTAC and C_{16} -CAR in pH 2 buffer. For both surfactants, the change in fluorescence intensity with varying concentrations of the surfactants was observed to be very small and irregular, and there was no spectral shift. From the ST measurement, we found that the pepsin–surfactant interaction in solution of pH 2 is weaker in nature, which is reflected by the fluorescence intensity profile. Also, at pH 5, the change in the fluorescence spectra of Trp residues (Figure S7) of pepsin in the absence and presence of C_{16} -CAR (or C_{16} -PTAC) is irregular in nature because, at this pH, charge neutralization causes precipitation of pepsin/surfactant complex from the solution. Therefore, pepsin–surfactant interactions could not be measured at this pH using the fluorescence technique. However, there is no doubt that the pepsin–surfactant interaction is very strong at pH 5. On the other hand, at pH 11, the protein transforms into a completely denatured state in which pepsin exists in the extended conformation; therefore, its affinity toward the substrate is less in this state. Figure S8 depicts the fluorescence spectra of pepsin in the absence and presence of both surfactants. For both surfactants, no shift of the fluorescence spectrum was observed, except about 10% increase of the fluorescence intensity. This means that the polarity of the microenvironments of the Trp residues does not change when the surfactant molecules interact with pepsin. The small increase of the fluorescence intensity might be a consequence of the conformational change of pepsin due to binding of the cationic surfactant molecules. The small change of fluorescence intensity, however, could not reliably be used to confirm surfactant binding to the pepsin at pH 11.

The fluorescence spectral change of pepsin upon interaction with the cationic surfactants is shown in Figure 4. As

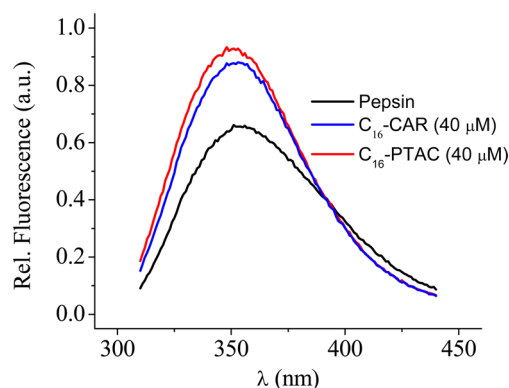


Figure 4. Fluorescence emission spectra of pepsin in phosphate buffer (20 mM, pH 8) in the absence and presence of C_{16} -CAR (40 μ M) and C_{16} -PTAC (40 μ M) at 25 $^{\circ}$ C.

mentioned before, the fluorescence intensity of pepsin at pH 8 is less compared to that at pH 5. This is because, in the I_p state of pepsin at pH 8, the hydrophobic residues including Trp residues are exposed to bulk water. However, the exposure of the hydrophobic residues enhances its tendency to aggregate formation, as has been demonstrated in our earlier work.⁴⁵ When a small amount of surfactant is added to the pepsin solution at pH 8, the surfactant molecules bind to the hydrophobic region of pepsin through the hydrophobic tail, and thus prevent aggregation of pepsin. Also, as a result of surfactant binding to the I_p state of pepsin, the Trp residues are again pushed to a less polar environment, as indicated by the increase of fluorescence intensity. In fact, pepsin is refolded to a new state upon addition of surfactant, which is confirmed by the change of CD spectra (see Figure S9 of the Supporting Information).

CD Spectra. The CD spectra of pepsin at different pHs in the presence as well as in the absence of surfactant molecules were recorded (Figure 5) in order to monitor the conformational changes, if any, that occurred due to surfactant binding. As indicated by the CD spectra in Figure 5a, none of the surfactant (C_{16} -CAR or C_{16} -PTAC) molecules caused any conformational change of pepsin at pH 2, which is consistent with the results of steady-state fluorescence measurements. At pH 5, however, the secondary structure of pepsin changed when it interacted with both surfactant molecules (Figure 5b), but the change is observed to be very small. In the alkaline denatured state (I_p), pepsin interacts with both C_{16} -CAR and C_{16} -PTAC surfactants, as manifested by the conformational changes of the protein. In the case of the pepsin/ C_{16} -PTAC complex, the conformational change is large as compared to C_{16} -CAR. There is a decrease of θ value which suggests a decrease of helicity and an increase of β -sheet or random coil structure. These may be due to the hydrophobic interaction between pepsin and C_{16} -PTAC. The increase of β -sheet structure indicates that the protein undergoes transformation to a new refolded state which is consistent with the fluorescence spectra (Figure 4). In the case of C_{16} -CAR, there is a $-OH$ group in the headgroup which increases the hydrophilicity as well as steric repulsion of the headgroup, and consequently, the pepsin– C_{16} -CAR interaction is less favorable. The small conformational change of pepsin can be clearly observed from the CD spectra, as shown in Figure 5c. At pH 11, on the other hand, there is a shift as well as a decrease of intensity of the CD spectrum when C_{16} -CAR (or C_{16} -PTAC) is added to the pepsin solution. As a result of interaction with the surfactant molecules, the electron density of the amide bonds in pepsin changes, causing a shift of the spectrum and reduction of intensity.

Time-Resolved Fluorescence Measurements. In order to study the conformational dynamics, the intrinsic fluorescence lifetime (τ_f) of pepsin was measured in the presence of surfactant molecules. At all of the pHs, pepsin exhibits biexponential fluorescence emission decays (see Figures S10–S13, Supporting Information) with two lifetime values (τ_1 and τ_2), the average value ($\langle\tau_f\rangle$) of which was calculated from $\langle\tau_f\rangle = f_1\tau_1 + f_2\tau_2$.³⁹ The data are collected in Table 1. In a solution of pH 2, the average lifetime ($\langle\tau_f\rangle$) value of pepsin does not change significantly upon addition of C_{16} -CAR or C_{16} -PTAC. This is probably because the surfactants either do not bind to pepsin or bind to a region far apart from the Trp residues of pepsin, which is consistent with the results of fluorescence and CD spectral measurements. Interestingly, when the pH is

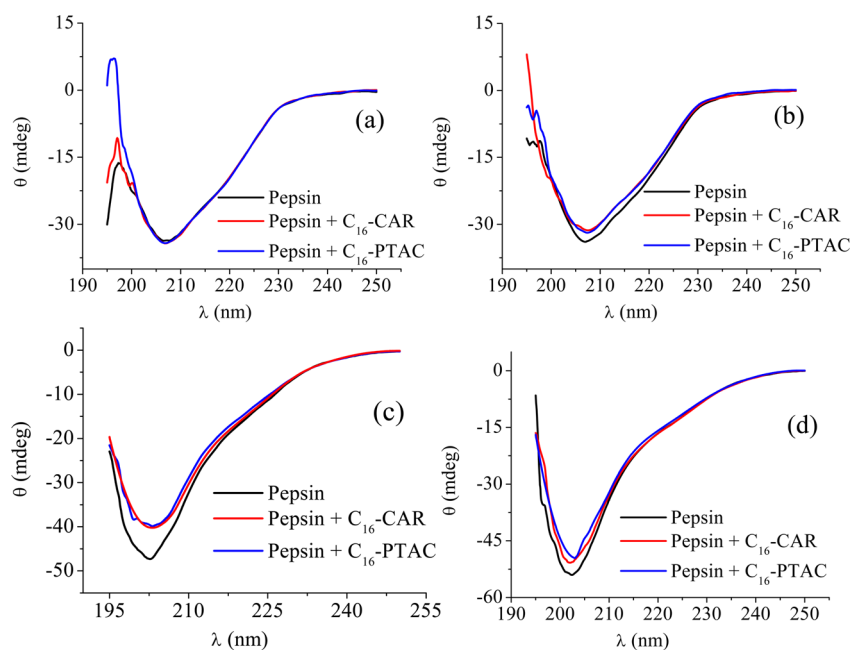


Figure 5. CD spectra of pepsin, pepsin/ C_{16} -CAR, and pepsin/ C_{16} -PTAC complexes in 20 mM phosphate buffer of (a) pH 2, (b) pH 5, (c) pH 8, and (d) pH 11 at 25 °C.

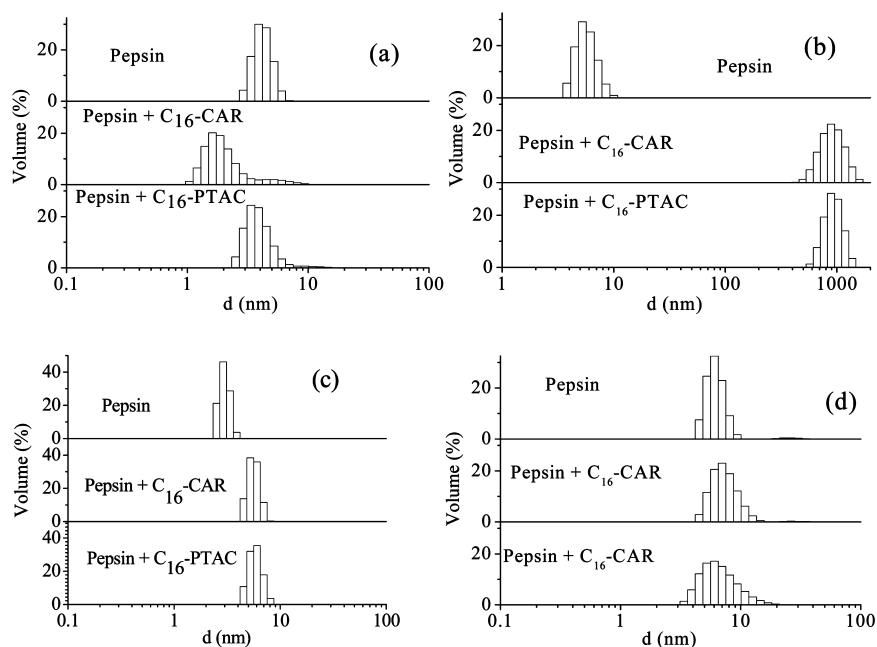


Figure 6. Size distribution histograms of pepsin and pepsin/surfactant complex in phosphate buffer (20 mM) of (a) pH 2, (b) pH 5, (c) pH 8, and (d) pH 11 at 25 °C; for pH 2, 8, and 11, $[C_{16}\text{-PTAC}] = [C_{16}\text{-CAR}] = 40 \mu\text{M}$; for pH 5, $[C_{16}\text{-PTAC}] = [C_{16}\text{-CAR}] = 20 \mu\text{M}$.

increased to 5, the $\langle\tau_f\rangle$ value increases, which means pepsin undergoes a conformational change to a more compact structure in which the Trp residues are buried within the protein structure. Upon addition of C_{16} -CAR or C_{16} -PTAC, the individual lifetime components as well as the $\langle\tau_f\rangle$ value decreased. This means that either there is a conformational change of pepsin as a result of surfactant binding or there is dynamic quenching of fluorescence. Since CD spectra do not exhibit any change, there is no substantial change occurring in the structure of the pepsin and the reduction of fluorescence lifetime must be due to dynamic quenching.

At pH 8, the $\langle\tau_f\rangle$ value of pepsin decreased as the Trp residues and the hydrophobic patches are exposed to bulk water as a result of partial denaturation. Though the surface charge of the pepsin is greater at pH 8, the surfactants mainly interact through hydrophobic interaction at this pH because the hydrophobic patches are available for surfactant binding. It is important to note that the lifetime of the slower component of pepsin at pH 8 upon interaction with C_{16} -CAR or C_{16} -PTAC remains almost unchanged, whereas the faster component changes with the addition of surfactant (see Table 1). This change in the lifetime may be attributed to the refolding of pepsin to a new state. This refolding is greater in the case of

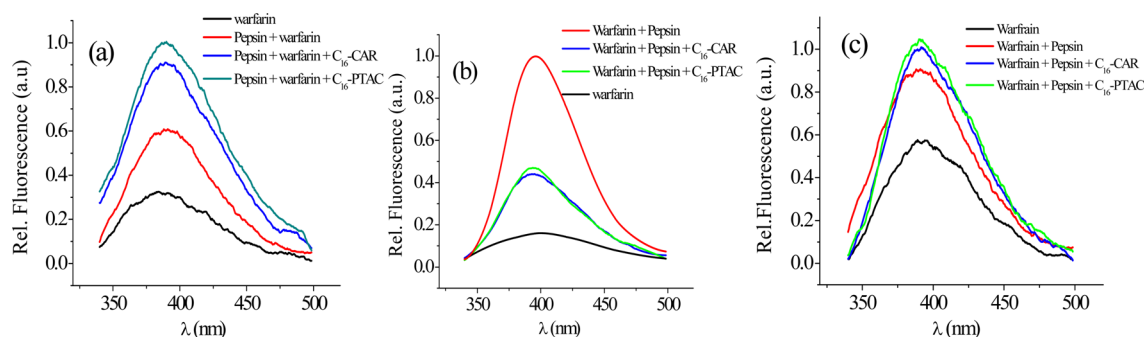


Figure 7. Fluorescence spectra of free and pepsin bound warfarin in the presence of C_{16} -CAR and C_{16} -PTAC surfactants ($40 \mu\text{M}$) in 20 mM phosphate buffer of (a) pH 5, (b) pH 8, and (c) pH 11 at $25 \text{ }^\circ\text{C}$.

C_{16} -PTAC due to its stronger hydrophobic interaction with pepsin compared to that of C_{16} -CAR as the pepsin exposes its hydrophobic region at pH 8. At pH 11, pepsin is in denatured condition, so the average lifetime of the pepsin decreases as the Trp residues are solvent exposed. At this pH, when C_{16} -CAR or C_{16} -PTAC is added to pepsin, the $\langle\tau_f\rangle$ value of Trp residues remains almost unchanged, which means no conformational change occurs at this pH upon addition of the surfactants.

Hydrodynamic Size of Pepsin/Surfactant Complexes. DLS is one of the most sensitive techniques to determine the hydrodynamic size and size distribution of particles in a colloidal dispersion. Since the hydrodynamic diameter of protein molecules is expected to increase upon surfactant binding, DLS can confirm protein/surfactant complex formation. The size distributions of pepsin at pH 2 obtained from DLS measurements show that the mean hydrodynamic diameter of pepsin is about 3 nm (Figure 6a). Upon interaction with both surfactant molecules, the size of pepsin remains almost the same, which means there is no interaction with the surfactant molecules at pH 2. In fact, from the results of CD and fluorescence measurements, we were also not able to confirm pepsin/surfactant complex formation at pH 2. At pH 5, the mean hydrodynamic diameter of pepsin increases to about 5 nm (Figure 6b) and when it interacts with C_{16} -CAR or C_{16} -PTAC ($20 \mu\text{M}$) the size of the complex increases to 900 nm. As already mentioned above, at higher surfactant concentrations ($>20 \mu\text{M}$), pepsin/surfactant complex precipitates out of the solution because the negative charge of the protein is completely neutralized. Therefore, the existence of large particles (900 nm) in the presence of low surfactant concentrations at pH 5 must be due to the precipitation of pepsin/surfactant complex. At pH 8 also, both of the surfactant molecules interact with the pepsin in the same manner and the mean hydrodynamic diameter of the protein is increased from 3 to 7 nm, as shown by the size distribution histograms in Figure 6c. At pH 11, the pepsin is in a denatured state and it is quite obvious that the hydrodynamic diameter ($\sim 6 \text{ nm}$) of pepsin is higher (Figure 6d). However, upon interaction with C_{16} -CAR (or C_{16} -PTAC) surfactant molecules, the size distribution gets broadened with a small increase of the mean hydrodynamic diameter of the pepsin/surfactant complex formed at pH 11, confirming the protein–surfactant interaction.

3.3. Determination of the Binding Site of C_{16} -CAR and C_{16} -PTAC. Warfarin is known to be a site marker for ligands that bind to BSA and HSA proteins.⁴⁶ Warfarin is known to bind to the drug binding site I in subdomain IIA of BSA (or HSA). In the case of pepsin, though, there is no known site marker and we used warfarin as a site marker. It may be

assumed that the warfarin binds to pepsin protein at a site where most small molecules bind. In this experiment, the warfarin concentration was kept constant at $1 \mu\text{M}$, and it was excited at 325 nm, where the Trp residues of pepsin have no absorption. As mentioned before, the N-terminal lobe of pepsin is more flexible at pH 2 and there is no interaction between pepsin and the surfactant molecules (see the ITC section). Therefore, we did not perform the site marker experiment at this pH. However, at pH 5, the intensity of the fluorescence spectrum of warfarin upon binding to pepsin (Figure 7a). In the presence of C_{16} -CAR or C_{16} -PTAC, the intensity of warfarin fluorescence is further enhanced. This means the microenvironment of the warfarin molecule becomes more hydrophobic upon interaction with the surfactant molecules. From the fluorescence spectra in Figure 7a, it is clear that warfarin is not replaced by C_{16} -CAR (or C_{16} -PTAC) and rather the surfactant molecules help binding of the warfarin molecule cooperatively. Thus, it can be concluded that the binding sites of warfarin and C_{16} -CAR (or C_{16} -PTAC) are different, but their binding to pepsin is cooperative in nature. In contrast, at pH 8, the fluorescence intensity of warfarin bound pepsin (Figure 7b) is partially reduced when C_{16} -CAR (or C_{16} -PTAC) is added to the solution. This means partial replacement of warfarin from its binding site as a result of surfactant binding. Thus, we can conclude that the warfarin and both surfactants share the same binding site of pepsin at pH 8. Both surfactants decreased the fluorescence intensity by the same extent at a given concentration. This is because both surfactants have the same hydrocarbon chain length. This means that the binding of surfactant molecules at this pH is hydrophobic in nature. As at pH 2, the fluorescence spectrum of warfarin bound pepsin did not change when C_{16} -CAR (or C_{16} -PTAC) surfactant was added to the pH 11 solution, which means that the binding pockets of warfarin and C_{16} -CAR (or C_{16} -PTAC) are different and their binding to pepsin is independent from one another. From the results of the site marker experiment, it can be concluded that the binding pockets for C_{16} -CAR or C_{16} -PTAC in pepsin are different at different pHs.

3.4. Binding Constants. As discussed before, the fluorescence spectrum of pepsin did not exhibit any significant change when the surfactant was added to the protein solution at pH 2, 5, and 11. Therefore, we failed to get any quantitative data for the binding efficiency of the surfactant at these pHs. This suggests that the binding efficiency of the cationic surfactants at these pHs is either weak or nil. The absence of surfactant binding at pH 11 is due to the denaturation of the protein resulting in an exposure of the substrate binding site

(i.e., the cleft between the C- and N-terminal lobes of the protein) to bulk water which is consistent with the earlier reports,⁴⁰ that suggested a decrease of substrate binding efficiency of pepsin with an increase of pH. The absence of any binding of C₁₆-CAR and C₁₆-PTAC surfactants to pepsin is demonstrated by the CD spectra (Figure 5).

Unlike pepsin solution in acidic pH (pH 2 and 5), the fluorescence intensity was observed to increase when the surfactant was added to the pepsin solution at pH 8, indicating binding of the surfactant molecules. In the literature, it has been associated with the removal of static quenching of the Trp residues upon binding of the surfactant with the ionized Asp and Glu residues of pepsin.^{47,48} At pH 8, the pepsin is in the partially unfolded I_p state in which the hydrophobic cleft of the protein is partially exposed to water. Upon addition of surfactant, the hydrocarbon tail of the surfactant penetrates into the cleft between the C- and N-terminal lobes of the protein through hydrophobic interactions, thus making the microenvironment of Trp residues less polar. Consequently, the intensity of pepsin fluorescence is enhanced. Moreover, the electrostatic interaction between the surfactant headgroup and the ionized Asp and/or Glu residue(s) removes the static quenching of the Trp fluorescence.

The fluorescence intensity data of pepsin at pH 8 were analyzed to determine the binding constant. Assuming n binding sites for a surfactant S on the protein P, the binding process can be represented as



$$K_b = \frac{[PS_n]}{[S]^n [P]} \quad (3)$$

where [S] and [P] are the free surfactant and protein concentrations, respectively, and [PS_n] is the concentration of the fluorophore/surfactant complex at equilibrium. As the fluorescence intensity increases with addition of surfactant

$$1/[P] \propto F \quad (4)$$

If [P]₀ is the total protein concentration, then

$$[P]_0/[P] = F/F_0 \quad (5)$$

Now,

$$[S] = [S]_0 - [PS_n] \quad (6)$$

and

$$[P]_0 = [P] + [PS_n] \quad (7)$$

Using eqs 5 and 7, we get

$$[PS_n] = \{(F - F_0)/F\}[P]_0 \quad (8)$$

Substituting eqs 5 and 8 in eq 3, we get

$$(K_b)^n = \{(F - F_0)/F_0\} \{1/[S]_0 - (F - F_0)[P]_0/F\}^n \quad (9)$$

Therefore,

$$\log\{(F - F_0)/F_0\} = n \log K_b - n \log\{1/[S]_0 - (F - F_0)[P]_0/F\} \quad (10)$$

The plots (Figure 8) of $\log\{(F - F_0)/F_0\}$ vs $\log\{1/[S]_0 - (F - F_0)[P]_0/F\}$ will give a straight line; from the slope and intercept, we can estimate the value of K_b and n . The binding

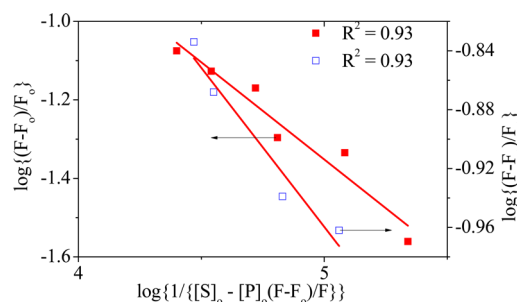


Figure 8. Plot of $\log\{(F - F_0)/F_0\}$ vs $\log\{1/[S]_0 - (F - F_0)[P]_0/F\}$ in phosphate buffer (20 mM, pH 8) at 25 °C: ■, C₁₆-PTAC; □, C₁₆-CAR.

constant of C₁₆-PTAC ($341.0 \pm 137.0 \text{ M}^{-1}$) is much larger than that of C₁₆-CAR ($3.15 \pm 0.55 \text{ M}^{-1}$). The weak or no binding of the latter is also indicated by the value of n (0.2) which is much less than that of C₁₆-PTAC (0.5) surfactant. As the structure of C₁₆-CAR is similar to that of C₁₆-PTAC, we can assume that both of the surfactants bind to the same pocket in pepsin. Since both surfactants have the same hydrocarbon tail, the surfactant headgroup plays an important role in the binding process. The very low K_b value for C₁₆-CAR must be due to the -OH group at the surfactant head which causes steric hindrance to surfactant binding and hence weakens the pepsin-C₁₆-CAR binding at pH 8. This means electrostatic interaction between the surfactant headgroup and the ionized Asp and/or Glu residues is the determining factor for the insertion of the hydrocarbon tail into the hydrophobic cleft between the C- and N-terminal lobes of the protein. In other words, the cationic surfactant molecules bind to the pepsin where the glutamate (Glu) and aspartate (Asp) residues are present.

3.5. Thermodynamics of Pepsin-Surfactant Interactions. The results of fluorescence studies indicate that surfactant binding to pepsin does not occur at pH 2, 5, and 11. However, these data should be treated carefully, as a change in the fluorescence spectra can be seen only when the substrate binding occurs near the Trp residue(s) of pepsin protein. That is, fluorescence is an indirect technique. Therefore, we have performed measurements using ITC which is a direct method for the determination of the binding constant. The latter method not only gives the binding constant value but also measures the relevant thermodynamic parameters, such as heat change (ΔH°), change of Gibbs free energy (ΔG°), and entropy change (ΔS°) for the binding process. Thermodynamic parameters characterizing ligand binding to proteins are important to account for the stability of the protein/surfactant complex as well as the mechanism of binding.

The thermodynamic parameters for the pepsin-surfactant interactions were determined at different pHs. The ITC thermograms of pepsin-C₁₆-CAR or pepsin-C₁₆-PTAC are presented in Figures S14, S15, S16, and S17. The corresponding binding data are included in Table 2. From the feature of the thermogram in Figure S14, we can see that the heat change is not significant, indicating that there is no interaction of pepsin with any of the cationic surfactants. This is because, at pH 2, the pepsin is almost charge neutral. Consequently, there is no electrostatic interaction between the positively charged surfactant molecule (C₁₆-CAR or C₁₆-PTAC) and neutral protein. Further, at this pH, pepsin is in its

Table 2. Values of Thermodynamic Parameters for Binding of C₁₆-CAR and C₁₆-PTAC Surfactants with Pepsin in 20 mM Phosphate Buffer (pH 5, 8, and 11) at 25 °C

pH	surfactants	ΔH° (kJ mol ⁻¹)	ΔS° (J K ⁻¹ mol ⁻¹)	ΔG° (kJ mol ⁻¹)	<i>n</i>	$K \times 10^{-3}$ (M ⁻¹)
5	C ₁₆ -CAR	-13.44 ± 0.92	29.82	-22.33	1	7.91 ± 0.36
		-97.36 ± 4.32	-256.62	-20.88	1	4.23 ± 0.22
	C ₁₆ -PTAC	8.23 ± 1.22	116.34	-26.44	1	41.3 ± 9.1
		327.60 ± 61.32	1155.00	-16.59	1	0.720 ± 0.14
8	C ₁₆ -CAR	135.16 ± 65.94	504.00	-15.03	1	0.517 ± 0.20
		-1302.84 ± 180.60	-4284.00	-26.20	1	5.43 ± 0.22
	C ₁₆ -PTAC	3.19 ± 0.20	104.16	-27.84	1	72.9 ± 6.10
		98.07 ± 6.72	389.76	-18.07	1	1.45 ± 0.11
11	C ₁₆ -CAR	12.93 ± 0.76	127.68	-25.11	11.60 ± 0.89	29.6 ± 11.0
	C ₁₆ -PTAC	2.95 ± 0.71	89.46	-23.70	8.68 ± 0.44	13.7 ± 7.85

native state and does not have any exposed hydrophobic patches and thus the hydrophobic interaction is nullified.

At pH 5, on the other hand, pepsin is in a stable conformation, but some of the Asp residues are deprotonated so it carries more negative charge compared to pH 2. Thus, we can expect some electrostatic interaction among the pepsin and C₁₆-CAR or C₁₆-PTAC. Since higher concentrations of surfactants caused precipitation as mentioned above, the ITC measurements were performed in the lower concentration range. From the data in Table 2, we can see that ΔG° is negative for both surfactants, which means that both surfactant molecules spontaneously bind to pepsin at this pH. Both C₁₆-CAR and C₁₆-PTAC exhibit sequential binding to two sets of binding sites in pepsin. For the first molecule of C₁₆-CAR, the ΔH° and ΔS° values suggest that the binding is enthalpy driven and the molecule binds to pepsin via H-bonding, van der Waals, and hydrophobic interaction. The -OH group present in the headgroup of C₁₆-CAR can interact with pepsin through H-bonding. However, the second molecule binds through H-bonding interaction, as the sign of both ΔH° and ΔS° is negative.⁴⁹ The C₁₆-CAR shows negative cooperativity when it binds to pepsin as the ΔG value becomes less negative when the second molecule binds to pepsin. A similar negative cooperativity is also observed with the C₁₆-PTAC surfactant. For the binding of the first molecule of C₁₆-PTAC, the value of ΔH° is very less positive and ΔS° has a very high positive value, indicating that the first molecule of C₁₆-PTAC interacts with pepsin via hydrophobic interaction. Unlike C₁₆-CAR, the second molecule of C₁₆-PTAC binds to pepsin only via hydrophobic interaction. In contrast to C₁₆-CAR, the hydrophobic interaction is much higher for the second molecule of C₁₆-PTAC in the absence of steric effects of the -OH group in the surfactant head. This means the -OH group plays a significant role in the binding of C₁₆-CAR to pepsin. It should also be noted that the binding efficiency for the second molecule of both C₁₆-CAR and C₁₆-PTAC is less than that for the first molecule.

The data in Table 2 suggest that, at pH 8, the binding pattern is different from that at pH 5. Both C₁₆-CAR and C₁₆-PTAC surfactants bind to pepsin at pH 8 in a sequential manner. Two molecules of C₁₆-CAR and C₁₆-PTAC bind to pepsin at this pH. For the first molecule, the binding of both C₁₆-CAR and C₁₆-PTAC is entropy driven, but for the second molecule, the binding process is enthalpy driven in the case of C₁₆-CAR and entropy driven in the case of C₁₆-PTAC. Also, in consistence with the fluorescence data, the binding efficiency for the first molecule is lower with C₁₆-CAR, but it is higher in the case of C₁₆-PTAC surfactant. For the second molecule, however, it is

just the opposite. The ΔH° and ΔS° values suggest that the binding of the first molecule of C₁₆-CAR occurs via a strong hydrophobic interaction accompanied by H-bonding interaction, but the second molecule of C₁₆-CAR binds to pepsin via H-bonding interaction only. This means there is a positive cooperativity for the stabilization of the pepsin/C₁₆-CAR complex. On the other hand, large positive values of both ΔH° and ΔS° in the case of C₁₆-PTAC, the first molecule binding occurs through hydrophobic interaction. For the second molecule, also the binding interaction is hydrophobic in nature, but it is entropy driven. Since pepsin is in the partially denatured state at this pH, the hydrophobic patches of pepsin are exposed and the hydrophobic interaction between the surfactant and the protein is expected. In the case of C₁₆-PTAC, negative cooperativity in binding of both of the molecules is observed. Thus, the -OH group in the C₁₆-CAR head must be responsible for the difference in binding pattern between the C₁₆-PTAC and C₁₆-CAR molecules.

From the data in Table 2, it can be concluded that, at pH 11, both surfactants bind to pepsin spontaneously and more efficiently. However, for both surfactants, the binding process is entropy driven. The small positive ΔH° values for both C₁₆-CAR and C₁₆-PTAC indicate that weak hydrophobic and strong electrostatic interactions are responsible for surfactant binding to pepsin protein. At pH 8, the hydrophobic interaction is observed to be the main driving force for the stabilization of the pepsin/surfactant complex, whereas, at pH 11, the electrostatic interaction is the main driving force. Since pepsin is completely denatured at this high pH and contains very high negative charge due to ionization of the buried Asp and Glu residues, a greater number of surfactant molecules can interact with the pepsin protein, as indicated by the large values of *n* for both surfactants. However, such binding occurs far away from the Trp residues and thus does not change their microenvironments, as indicated by the results of fluorescence studies. The complete unfolding of the protein at pH 11 also increases the binding efficiency of C₁₆-CAR, as there is no longer any steric hindrance for the surfactant headgroup.

4. CONCLUSIONS

First, we have studied the solution behavior of pepsin at different pHs. Pepsin is a β -sheet-rich protein and has been shown to remain in the rigid globular state at pH 5. The protein exists in the partially denatured state at pH 8, in which the N-terminal lobe becomes more flexible and, consequently, its surface activity increased. At pH 11, however, it is completely denatured. The increased surface activity of pepsin with the increase of pH above 5 is a result of ionization of the -COOH

groups of Asp and Glu residue(s) which increases flexibility of the molecular structure of pepsin. For the first time, we have shown that the N-terminal lobe of pepsin undergoes a conformational change below pH 5. Although pepsin is expected to be in the N_p state at pH 2, partial unfolding of the N-terminal lobe produces an acid-denatured state, D_p .

Second, the interaction of pepsin with two different cationic surfactants which differ from each other only in their headgroup structure was investigated. Although results of fluorescence studies did not indicate any interaction of these surfactants with pepsin at pH 2, 5, and 11, the ITC measurements resulted in binding data at all pHs, except pH 2. The interaction of pepsin with the two chosen cationic surfactants, C_{16} -CAR and C_{16} -PTAC, changes with the pH of the solution. In fact, the patterns of interaction of the cationic surfactants are similar at pH 5. At pH 8, the two surfactants under study bind to the pepsin near the glutamate (Glu) and aspartate (Asp) residues and also to the substrate binding site that is the cleft between the C- and N-terminal lobes of the protein. The binding efficiency of C_{16} -PTAC is greater than that of C_{16} -CAR at all pHs employed in this investigation, which means the $-OH$ group at the head of the C_{16} -CAR surfactant weakens pepsin-surfactant interaction due to steric hindrance. The effect of headgroup structure on surfactant binding to BSA protein has also been reported in the literature.^{50,51} The binding interactions are hydrophobic in nature at lower pHs (5 and 8), but at higher pH (11), the binding occurs mainly via electrostatic interaction. The binding constant of C_{16} -PTAC at pH 8 was observed to be greater than that at pH 5 and has been attributed to partial exposure of the hydrophobic cleft between the C- and N-terminal lobes of the protein. At pH 11, since the protein is completely unfolded, a large number of C_{16} -CAR (or C_{16} -PTAC) molecules bind to pepsin to sites far away from the Trp residues via electrostatic and hydrophobic interactions. The increase of binding efficiency for C_{16} -CAR is indicated by the increase of binding constant value in going from pH 8 to 11.

■ ASSOCIATED CONTENT

Supporting Information

The Supporting Information is available free of charge on the ACS Publications website at DOI: 10.1021/acs.jpcc.5b07072.

Details about the synthesis of surfactants, representative 1H NMR and ^{13}C NMR spectra of C_{16} -CAR and C_{16} -PTAC in $CDCl_3$, the fluorescence emission spectra of pepsin and pepsin bound C_{16} -CAR and C_{16} -PTAC at pH 2, 5, and 11, CD spectra of pepsin, fluorescence decay plots, and ITC plots at different pHs (PDF)

■ AUTHOR INFORMATION

Notes

The authors declare no competing financial interest.

■ ACKNOWLEDGMENTS

We thank Indian Institute of Technology Kharagpur for partial support of this work. S.G. thanks UGC, New Delhi, for the research fellowship (ref: F.No. 2-16/98(SA-1)). We thank Dr. N. Sarkar for the ζ -potential and DLS measurements.

■ REFERENCES

(1) Liu, C. L.; Kamei, D. T.; King, J. A.; Wang, D. I. C.; Blankschtein, D. Separation of proteins and viruses using two-phase aqueous micellar systems. *J. Chromatogr., Biomed. Appl.* **1998**, *711*, 127–138.

(2) Saitoh, T.; Tani, H.; Kamidate, T.; Watanabe, H. Phase separation in aqueous micellar solutions of nonionic surfactants for protein separation. *TrAC, Trends Anal. Chem.* **1995**, *14*, 213–217.

(3) Reynolds, J. A.; Tanford, C. Chemistry and metabolism of macromolecules. *J. Biol. Chem.* **1970**, *245*, 5161–5165.

(4) Tanford, C. Hydrophobic free energy, micelle formation and the association of proteins with amphiphiles. *J. Mol. Biol.* **1972**, *67*, 59–74.

(5) Shirahama, K.; Tsujii, K.; Takagi, T. Free-boundary electrophoresis of sodium dodecyl sulfate-protein polypeptide complexes with special reference to SDS-polyacrylamide gel electrophoresis. *J. Biochem. (Tokyo)* **1974**, *75*, 309–314.

(6) Jones, M. N.; Manley, P. Binding of n-alkyl sulphates to lysozyme in aqueous solution. *J. Chem. Soc., Faraday Trans. 1* **1979**, *75*, 1736–1744.

(7) Griffiths, P. C.; Roe, J. A.; Bales, B. L.; Pitt, A. R.; Howe, A. M. Fluorescence probe studies of gelatin-sodium dodecyl sulfate interactions. *Langmuir* **2000**, *16*, 8248–8254.

(8) Otzen, D. Protein-surfactant interactions: A tale of many states. *Biochim. Biophys. Acta, Proteins Proteomics* **2011**, *1814*, 562–591.

(9) Randolph, T. W.; Jones, L. S. Surfactant-protein interactions. In *Rational design of stable protein formulations*; Carpenter, J. F., Manning, M., Eds.; Kluwer Academic/Plenum Publishers: New York, 2002; pp 159–175.

(10) Jones, M. N. Protein-surfactant interactions. In *Surface activity of proteins*; Magdassi, S., Ed.; Marcel Dekker: New York, 1996; pp 237–284.

(11) Tanford, C. *The hydrophobic effect. Formation of micelles and biological membranes*, 2nd ed.; Wiley & Sons: New York, 1980.

(12) Steinhardt, J. The nature of specific and non-specific interactions of detergents with proteins: Complexing and unfolding. In *Protein-Ligand Interactions*; Sund, H., Blauer, G., Eds.; Walter de Gruyter, University of Konstanz: Berlin, Germany, 1975; pp 412–426.

(13) Nieto-Ortega, B.; Hierrezuelo, J.; Ruiz, C. C.; Navarrete, J. T. L.; Casado, J.; Ramirez, F. J. Unfolding pathway of a globular protein by surfactants monitored with raman optical activity. *J. Phys. Chem. Lett.* **2014**, *5*, 8–13.

(14) De, D.; Santra, K.; Datta, A. Prototropism of [2,2'-Bipyridyl]-3,3'-diol in albumin-SDS aggregates. *J. Phys. Chem. B* **2012**, *116*, 11466–11472.

(15) Stenstam, A.; Khan, A.; Wennerstrom, H. The lysozyme-dodecyl sulfate system. an example of protein-surfactant aggregation. *Langmuir* **2001**, *17*, 7513–7520.

(16) Liu, W.; Guo, X.; Guo, R. The interaction between hemoglobin and two surfactants with different charges. *Int. J. Biol. Macromol.* **2007**, *41*, 548–557.

(17) Tofani, L.; Feis, A.; Snoko, R. E.; Berti, D.; Baglioni, P.; Smulevich, G. Spectroscopic and interfacial properties of myoglobin/surfactant complexes. *Biophys. J.* **2004**, *87*, 1186–1195.

(18) Ghosh, S.; Banerjee, A. A multitechnique approach in protein/surfactant interaction study: physicochemical aspects of sodium dodecyl sulfate in the presence of trypsin in aqueous medium. *Biomacromolecules* **2002**, *3*, 9–16.

(19) Ghosh, S. Interaction of sodium dodecyl sulfate (SDS) with two globular proteins (trypsin and papain) in aqueous medium. *J. Surf. Sci. Technol.* **2003**, *19*, 167–181.

(20) Ghosh, S. Physicochemical and conformational studies of papain/sodium dodecyl sulfate system in aqueous medium. *Colloids Surf., A* **2005**, *264*, 6–161.

(21) Nielsen, A. D.; Borch, K.; Westh, P. Thermochemistry of the specific binding of C12 surfactants to bovine serum albumin. *Biochim. Biophys. Acta, Protein Struct. Mol. Enzymol.* **2000**, *1479*, 321–331.

(22) Otzen, D. E.; Sehgal, P.; Westh, P. α -Lactalbumin is unfolded by all classes of detergents but with different mechanisms. *J. Colloid Interface Sci.* **2009**, *329*, 273–283.

(23) Lundahl, P.; Greijer, E.; Sandberg, M.; Cardell, S.; Eriksson, K.-O. A model for ionic and hydrophobic interactions and hydrogen-bonding in sodium dodecyl sulfate-protein complexes. *Biochim. Biophys. Acta, Protein Struct. Mol. Enzymol.* **1986**, *873*, 20–26.

- (24) Gull, N.; Chodankar, S.; Aswal, V. K.; Sen, P.; Khan, R. H.; Kabir-ud-Din. Spectroscopic studies on the interaction of cationic surfactants with bovine serum albumin. *Colloids Surf., B* **2009**, *69*, 122–128.
- (25) Sun, C.; Yang, J.; Wu, X.; Huang, X.; Wang, F.; Liu, S. Unfolding and refolding of bovine serum albumin induced by cetylpyridinium bromide. *Biophys. J.* **2005**, *88*, 3518–3524.
- (26) Madaeni, S. S.; Rostami, E. Spectroscopic investigation of the interaction of BSA with cationic surfactants. *Chem. Eng. Technol.* **2008**, *31*, 1265–1271.
- (27) Kun, R.; Kis, L.; Dékány, I. Hydrophobization of bovine serum albumin with cationic surfactants with different hydrophobic chain length. *Colloids Surf., B* **2010**, *79*, 61–68.
- (28) Gospodarczyk, W.; Szutkowski, K.; Kozak, M. Interaction of bovine serum albumin (BSA) with novel gemini surfactants studied by synchrotron radiation scattering (SR-SAXS), circular dichroism (CD), and nuclear magnetic resonance (NMR). *J. Phys. Chem. B* **2014**, *118*, 8652–8661.
- (29) Wang, Y.; Jiang, X.; Zhou, L.; Yang, L.; Xia, G.; Chen, Z.; Duan, M. Synthesis and binding with BSA of a new gemini surfactant. *Colloids Surf., A* **2013**, *436*, 1159–1169.
- (30) Tai, S.; Liu, X.; Chen, W.; Gao, Z.; Niu, F. Spectroscopic studies on the interactions of bovine serum albumin with alkyl sulfate gemini surfactants. *Colloids Surf., A* **2014**, *441*, 532–538.
- (31) Mir, M. U. H.; Maurya, J. K.; Ali, S.; Ubaid-ullah, S.; Khan, A. B.; Patel, R. Molecular interaction of cationic gemini surfactant with bovine serum albumin: A spectroscopic and molecular docking study. *Process Biochem.* **2014**, *49*, 623–630.
- (32) Tang, J.; Sepulveda, P.; Marciszyn, J., JR; Chen, K. C. S.; Huang, W.-Y.; Tao, N.; Liu, D.; Lanier, J. P. Amino-acid sequence of porcine pepsin. *Proc. Natl. Acad. Sci. U. S. A.* **1973**, *70*, 3437–3439.
- (33) Pande, M.; Kumari, N. K. P.; Dubey, V. K.; Tripathi, P.; Jagannadham, M. V. Stability and unfolding studies on alkaline denatured state (Ip) of pepsin. *Process Biochem.* **2009**, *44*, 906–911.
- (34) Zhang, H.; Cao, J.; Fei, Z.; Wang, Y. Investigation on the interaction behavior between bisphenol A and pepsin by spectral and docking studies. *J. Mol. Struct.* **2012**, *1021*, 34–39.
- (35) Huang, Y.; Yan, J.; Liu, B.; Yu, Z.; Cao, X.; Tang, Y.; Zi, Y. Investigation on interaction of prulifloxacin with pepsin: A spectroscopic analysis. *Spectrochim. Acta, Part A* **2010**, *75*, 1024.
- (36) Chakraborty, T.; Chakraborty, I.; Moulik, S. P.; Ghosh, S. Physicochemical studies on pepsin–CTAB interaction: Energetics and structural changes. *J. Phys. Chem. B* **2007**, *111*, 2736–2746.
- (37) Boeris, V.; Micheletto, Y.; Lionzo, M.; Pesce da Silveira, N.; Picó, G. Interaction behavior between chitosan and pepsin. *Carbohydr. Polym.* **2011**, *84*, 459–464.
- (38) Patra, T.; Ghosh, S.; Dey, J. Cationic vesicles of a carnitine-derived single-tailed surfactant: Physicochemical characterization and evaluation of in vitro gene transfection efficiency. *J. Colloid Interface Sci.* **2014**, *436*, 138–145.
- (39) Lakowicz, J. R. *Principles of fluorescence spectroscopy*; Plenum Press: New York, 1983.
- (40) Campos, L. A.; Sancho, J. Interaction behavior between chitosan and pepsin. *FEBS Lett.* **2003**, *538*, 89–95.
- (41) Kim, S. H.; Kinsella, J. E. Surface active properties of proteins: Effects of progressive succinylation on film properties and foam stability of glycinin. *J. Food Sci.* **1987**, *52*, 1341–1343.
- (42) Herriott, R. M. Pepsinogen and pepsin. *J. Gen. Physiol.* **1962**, *45*, 57–76.
- (43) Privalov, P. L.; Mateo, P. L.; Khechinashvili, N. N.; Stepanov, V. M.; Revina, L. P. Comparative thermodynamic study of pepsinogen and pepsin structure. *J. Mol. Biol.* **1981**, *152*, 445–464.
- (44) Surewicz, W. K.; Mantsch, H. H.; Chapman, D. Determination of protein secondary structure by Fourier transform infrared spectroscopy: A critical assessment. *Biochemistry* **1993**, *32*, 389–394.
- (45) Ghosh, S.; Dolai, S.; Dey, J. Amyloid fibril formation by pepsin in neutral pH at room temperature. *Soft Matter* **2013**, *9*, 11457–11460.
- (46) Zhang, Y.-Z.; Zhou, B.; Zhang, X.-P.; Huang, P.; Li, C.-H.; Liu, Y. Interaction of malachite green with bovine serum albumin: Determination of the binding mechanism and binding site by spectroscopic methods. *J. Hazard. Mater.* **2009**, *163*, 1345–1352.
- (47) Gelamo, E. L.; Silva, C. H. T. P.; Imasato, H.; Tabak, M. Interaction of bovine (BSA) and human (HSA) serum albumins with ionic surfactants: Spectroscopy and modeling. *Biochim. Biophys. Acta, Protein Struct. Mol. Enzymol.* **2002**, *1594*, 84–99.
- (48) Gelamo, E. L.; Tabak, M. Spectroscopic studies on the interaction of bovine (BSA) and human (HSA) serum albumins with ionic surfactants. *Spectrochim. Acta, Part A* **2000**, *56*, 2255–2271.
- (49) Ross, P. D.; Subramanian, S. Thermodynamics of protein association reactions: Forces contributing to stability. *Biochemistry* **1981**, *20*, 3096–3102.
- (50) Ghosh, S.; Dey, J. Binding of fatty acid amide amphiphiles to bovine serum albumin: Role of amide hydrogen bonding. *J. Phys. Chem. B* **2015**, *119*, 7804–7815.
- (51) Ghosh, S.; Dey, J. Interaction of bovine serum albumin with N-acyl amino acid based anionic surfactants: Effect of head-group hydrophobicity. *J. Colloid Interface Sci.* **2015**, *458*, 284–292.